Published in final edited form as:
Heart Rhythm. 2012 January ; 9(1): 96–104. doi:10.1016/j.hrthm.2011.08.024.

Ionic Mechanism of Shock-Induced Arrhythmias: Role of Intracellular Calcium

Brittany Sowell, BS and **Vladimir G. Fast, PhD**
Department of Biomedical Engineering, University of Alabama at Birmingham, Birmingham, AL

Abstract

Background—Strong electrical shocks can cause focal arrhythmias, the mechanism of which is not well known. As shown previously, strong shocks produce diastolic Ca_i^{2+} increase, which may initiate focal arrhythmias via spontaneous Ca_i^{2+} rise (SCR), activation of inward Na^+-Ca^{2+} exchange current (I_{NCX}), and rise in membrane potential (V_m). It can be hypothesized that this mechanism is responsible for generation of shock-induced arrhythmias.

Objective—To examine the roles of SCRs and I_{NCX} in shock-induced arrhythmias.

Methods and Results—The occurrence of SCRs during shock-induced arrhythmias was assessed in neonatal rat myocyte cultures. Simultaneous V_m-Ca_i^{2+} optical mapping at arrhythmia source demonstrated that V_m upstrokes always preceded Ca_i^{2+} transients, and V_m-Ca_i^{2+} delays were not different between arrhythmic and paced beats (5.5±0.9 and 5.7±0.4 ms, respectively, p=0.5). Shocks caused gradual rise of diastolic Ca_i^{2+} consistent with membrane electroporation but no significant Ca_i^{2+} rises immediately before V_m upstrokes. Application of Ca_i^{2+} chelator BAPTA-AM (10 μmol/L) decreased the duration of shock-induced arrhythmias whereas application of I_{NCX} inhibitor KB-R7943 (2 μmol/L) increased it indicating that, despite the absence of SCRs, changes in Ca_i^{2+} affected arrhythmias. It is hypothesized that this effect is mediated by Ca_i^{2+} inhibition of outward I_{K1} current and destabilization of resting V_m. Possible I_{K1} role was supported by application of I_{K1} inhibitor $BaCl_2$ (0.2 mmol/L), which increased the arrhythmia duration.

Conclusions—Shock-induced arrhythmias in neonatal rat myocyte monolayers are not caused by spontaneous Ca_i^{2+} rises and inward I_{NCX}. However, these arrhythmias depend on Ca_i^{2+} changes, possibly via Ca_i^{2+}–dependent modulation of outward I_{K1} current.

Keywords

defibrillation; membrane potential; intracellular calcium; optical mapping

INTRODUCTION

Defibrillation is currently the only reliable method to halt life-threatening ventricular fibrillation (VF),[1] but electrical shocks may cause adverse effects including pain, tissue damage, decreased cardiac output, and arrhythmias.[2,3] This last effect is important because

Correspondence: Vladimir G. Fast, PhD, University of Alabama at Birmingham, 1670 University Blvd., VH B126, Birmingham, AL 35294, Phone: 205-975-2119, Fax: 205-975-4720, fast@crml.uab.edu.

arrhythmias may cause VF re-initiation[4,5] or induction of atrial fibrillation.[6] The ionic mechanism of shock-induced arrhythmias is not well known. It has been shown that strong shocks may cause membrane electroporation,[7,8] which can potentially lead to arrhythmias via two different ionic mechanisms. In one mechanism, arrhythmias are caused by increase in membrane conductance[9] and inward flow of a non-specific leakage current. This current may elevate diastolic V_m,[10–12] bringing it toward activation threshold and causing premature action potentials and arrhythmias.

In the other mechanism, arrhythmias may be caused by shock-induced increase of diastolic intracellular calcium concentration (Ca_i^{2+} overload).[11,13] It is well established that Ca_i^{2+} overload can be arrhythmogenic, and it is considered one of the main causes of focal arrhythmias. A common scenario for development of such arrhythmias involves V_m-independent rise of Ca_i^{2+} due to spontaneous calcium release from the sarcoplasmic reticulum, followed by activation of a transient inward current, which causes V_m elevation, abnormal action potentials, and arrhythmias.[14] The most likely candidate for the role of the transient inward current is the Na^+-Ca_i^{2+} exchange (NCX) current.[15,16] The singular feature of this arrhythmic mechanism is the spontaneous Ca_i^{2+} rise (SCR) which precedes or coincides with the rise in V_m. Such SCRs were observed in several animal models of arrhythmias,[17–20] but the role of this mechanism in shock-induced arrhythmias remains unknown.

The main purpose of this study was to use simultaneous optical mapping of V_m and Ca_i^{2+} to examine the role of spontaneous Ca_i^{2+} rises in a cell culture model of shock-induced arrhythmias,[7,10] which allows localization of the arrhythmia source. In addition, channel inhibitors were used to assess the roles of ion currents in these arrhythmias.

METHODS

Cell cultures

The research protocol was approved by the Institutional Animal Care and Use Committee. Patterned growth substrates for cell strands with defined geometries were fabricated using previously published procedures.[21] Two types of growth patterns were used: 0.15-mm wide strands containing square 0.8-mm wide expansions (Figure 1A), and linear 0.8-mm wide strands (Figure 1B). Primary cardiomyocytes were obtained from 1- to 2-day old Sprague-Dawley rats (Harlan) according to previously published procedures.[22] Cells were grown in Ultraculture serum-free medium (BioWhittaker) supplemented with antibiotics, 2 μg/ml vitamin B_{12}, 0.5 μmol/L epinephrine, and 0.1 mol/L bromodeoxyuridine, and incubated at 37°C in a humidified atmosphere containing 4.5% CO_2. Medium was exchanged the day after culture preparation and every second day thereafter. Experiments were performed between 3 and 10 days in culture.

Optical mapping of V_m and Ca_i^{2+} at the arrhythmia source

These experiments were performed in narrow strands with square expansions (Figure 1C), which allowed mapping and localization of the arrhythmia source.[10] V_m and Ca_i^{2+} changes were measured using an optical mapping technique described previously[23] with some modifications. Cells were double-stained with V_m-sensitive dye RH-237 and Ca_i^{2+}-sensitive dye Rhod-2 or Fluo-3. First, cells were stained with either 2.5 μmol/L of Rhod-2 for 40 minutes or 5 μmol/L of Fluo-3 for one hour in the incubator. To enhance Fluo-3 retention, 1 mmol/L probenecid was added to the Hanks solution.[23] Then, monolayers were transferred to an experimental chamber, superfused with Hanks solution (Sigma) with pH of 7.4 and temperature of 35–36°C, and stained with 4 μmol/L of RH-237 for 6 minutes. Rhod-2 and Fluo-3 are high-affinity dyes that overestimate the duration of Ca_i^{2+} transients in cell

cultures.[13] They were used instead of their low-affinity analogs because simultaneous V_m-Ca_i^{2+} measurements with low-affinity dyes resulted in low signal-to-noise ratio. The main focus in the present study was on the relationship between V_m and Ca_i^{2+} upstrokes. As shown previously,[13] the timing of Ca_i^{2+} upstroke is unaffected by dye affinity.

Fluorescence was measured using two 16×16-element photodiode arrays (Hamamatsu) and a microscopic mapping system[22] with spatial resolution of 110 μm/diode. For the Rhod-2/RH-237 dye combination, fluorescence was excited using a 200-W Hg/Xe lamp at 530/40 nm and measured at 580/40 nm (Rhod-2) and >710 nm (RH-237). For the Fluo-3/RH-237 dye combination, fluorescence was excited at 530/40 nm and measured at 580/40 nm (Fluo-3) and >680 nm (RH-237). Initial measurements were performed with the Rhod-2/RH-237 dye combination. Such recordings had excellent Ca_i^{2+} signal quality but rather low V_m signal-to-noise ratio. Therefore, subsequent measurements were performed using the Fluo-3/RH-237 combination, for which signal quality was similar for V_m and Ca_i^{2+} signals.

To reduce dye bleaching and phototoxicity, V_m-Ca_i^{2+} recordings were limited to 1-sec duration. Cells were paced at a cycle length of 500 ms. A control optical recording was taken without shock application to check for absence of spontaneous activity. In such quiescent strands, rectangular uniform-field shocks with 10-ms duration were delivered via two platinum plate electrodes. The field strength (*E*) was measured using a bipolar electrode. Shock delivery was synchronized with stimulation pulses. Because shocks occur during different phases of action potentials in different parts of cell strands, the effect of shock timing on arrhythmia induction was examined by applying shocks with strength of ~38 V/cm with coupling intervals of 30, 80, 130, 230, and 430 ms in 6 linear cell strands from 3 monolayers. Results showed that arrhythmia duration for longer coupling intervals did not differ from that for the 30-ms interval (data not shown). Therefore, the 30-ms coupling interval was used in all experiments, which resulted in the AP-shock delay of 15–25 ms. Shocks were applied with a strength just above the arrhythmia induction threshold (E~20–35 V/cm) because such shocks produced arrhythmias with a relatively long cycle length, which reduced interference from motion artifact in analysis of V_m-Ca_i^{2+} relationships during arrhythmic beats. Only those arrhythmic episodes were analyzed in which the earliest activation site was inside the expansion area. AP and Ca_i^{2+} transient rise times were measured at 50% of respective signal amplitudes. These measurements were used to calculate V_m-Ca_i^{2+} delays.

Effects of drugs on shock-induced arrhythmias

These experiments were performed in 0.8-mm wide strands (Figure 1D), in which shock-induced arrhythmias were previously extensively characterized[7,10,13] and which have more reproducible width than the local expansions. To examine the role of Ca_i^{2+} in shock-induced arrhythmias, arrhythmia duration was measured in control monolayers and monolayers treated with Ca_i^{2+} chelator BAPTA-AM applied at 10-μmol/L concentration for 40 minutes. To monitor arrhythmias, cells were stained with 2.5 μmol/L of RH-237 for 5 minutes. To minimize dye photobleaching and phototoxicity, fluorescent recordings were performed at 10% of the normal excitation light intensity and recording duration was limited to 5 sec. Extensive temporal signal filtration and spatial averaging were used to improve signal-to-noise ratio. Shocks with strengths of 0, 10, 20, and 30 V/cm were used to induce arrhythmias.

To examine the roles of ionic currents in shock-induced arrhythmias, two inhibitors were applied: the I_{NCX} blocker KB-R7943 at 2-μmol/L concentration and the I_{K1} inhibitor $BaCl_2$ at 0.2-mmol/L concentration. Arrhythmias were recorded using 5-sec recordings of cell contractions in transmitted light during application of shocks with strength of 0, 10, 20, 30 and 40 V/cm. Each series of measurements was performed at the same location three times:

before drug application (control), after 10-min drug application, and after 20-min drug washout.

Data were reported as mean±SD. Differences between means of two groups of data were compared using the 2-tailed paired or unpaired Student's t-test. Differences between three groups of data were compared using ANOVA test followed by post-hoc t-test with Bonferroni correction. Results were considered statistically significant if $p<0.05$.

RESULTS

Optical mapping of V_m and Ca_i^{2+} at the arrhythmia source

Arrhythmic beats with a localized source were mapped in 14 strands with local expansions from 9 monolayers. Figure 2A illustrates the effects of a shock with strength of 29 V/cm on V_m and Ca_i^{2+} in one cell strand. The shock induced one arrhythmic beat with cycle length of ~380 ms. Also shown are the activation pattern of the paced beat (Figure 2B), and the spatial distribution of shock-induced polarization (ΔV_m) across the expansion (Figure 2C), with maximal hyperpolarization on the left and maximal depolarization on the right.

Figure 3 illustrates activation maps of the arrhythmic beat and the correspondence between V_m and Ca_i^{2+} upstrokes at the arrhythmia source. The region of the earliest activation defined within the first 0.5 ms of activation times was not highly localized, but it was inside the expansion region (Figure 3A), indicating that the source of the arrhythmic beat was within this area. The spatial pattern of Ca_i^{2+} rise (Figure 3B) shows that the earliest Ca_i^{2+} rise was also within the square expansion. At all recording sites inside the expansion, Ca_i^{2+} rise followed the V_m rise (Figure 3C). Previously it was shown that spontaneous Ca_i^{2+} transients at the arrhythmia source may precede or follow V_m upstrokes with a much shorter delay than during paced beats.[17,19] Here, in contrast, the temporal relationship between V_m and Ca_i^{2+} rises in the area of earliest activation during the arrhythmic beat was not different from the paced beat. The average V_m-Ca_i^{2+} delay for the arrhythmic and the paced beats in this case was 5.8±1.4 ms and 6.0±0.4 ms, respectively.

Similar results were obtained for all arrhythmic episodes produced in strands with identifiable arrhythmia source by shocks with average strength of 30.2±6.1 V/cm (n=14), which produced 1–2 arrhythmic beats within 1-sec recording interval. In every arrhythmic beat, V_m upstrokes preceded Ca_i^{2+} transients at all recording sites. The average V_m-Ca_i^{2+} delay in the area of earliest activation during arrhythmic beats was 5.5±0.9 ms (Figure 3D), which was similar to that measured at the same sites during paced beats, which was 5.7±0.4 ms (n=14, NS).

Diastolic Ca_i^{2+} and V_m changes

It has been previously shown that relatively slow spontaneous Ca_i^{2+} rises during diastole may precede AP upstrokes and the following Ca_i^{2+} transients.[18] To analyze the effects of shocks on diastolic Ca_i^{2+} and V_m, optical recordings taken during shock application were compared to control recordings in 8 strands (in other six cases sufficiently long control recordings were not taken). Such comparison allowed elimination of signal changes caused by dye photobleaching and cell motion. Figure 4A illustrates an isochronal map of shock-induced diastolic V_m changes during application of a 29-V/cm shock as well as selected traces from control recordings (blue), shock recordings (green), and the difference between them (red). Because of relatively low V_m signal quality in these measurements, signals from nine diodes (3×3) were spatially averaged. At all sites, V_m was elevated following shock application as compared to control recordings. The magnitude of depolarization measured 10 ms prior to the earliest activation time of the arrhythmic AP (dashed line) was larger in the hyperpolarized area (49 %APA at site 1) than in the depolarized area (34 %APA at site

3) and the narrow strand (27 %APA at site 4). Analysis of diastolic depolarization in other strands showed similar results. Average diastolic V_m rise was higher in hyperpolarized areas than in depolarized areas (41.6±10 %APA versus 31.5±7 %APA, $p<0.05$) and narrows strands (28.6±13 %APA, $p<0.05$).

Figure 4B shows a map of diastolic Ca_i^{2+} increases, which was qualitatively similar to the V_m pattern inside the expansion. Also shown are raw Ca_i^{2+} traces from control and shock recordings, and the difference between them. It can be seen from the difference traces that the shock caused gradual diastolic Ca_i^{2+} elevation, which started right after shock application. The slope of diastolic Ca_i^{2+} elevation was relatively constant without additional rise preceding the arrhythmic AP. Such gradual Ca_i^{2+} elevation can be attributed to Ca^{2+} influx through shock-induced pores. Similar to V_m changes, the magnitude of diastolic Ca_i^{2+} elevation was larger in the area of shock-induced hyperpolarization (37 %CaA, site 1) than in the area of depolarization (25 %CaA, site 3) and in the narrow strand (21 %CaA, site 4), which is consistent with previous measurements of shock-induced Ca_i^{2+} changes in cell strands using low-affinity Ca_i^{2+} dye.[13] Similar differences were observed in other measurements. On average, diastolic Ca_i^{2+} elevation was 27.6±8, 14.3±7 and 8.1±9 %CaA in areas of maximal hyperpolarization, depolarization, and in narrow strands, respectively ($p<0.05$ for all comparisons). These values likely overestimate diastolic Ca_i^{2+} changes, however, due to non-linear response of high-affinity Ca_i^{2+} dyes used here.[13]

Effect of Ca_i^{2+} buffering on shock-induced arrhythmias

These experiments were performed in 17 strands from 5 monolayers treated with BAPTA-AM and 9 strands from 3 control monolayers. Figure 5A illustrates spatially and temporally filtered V_m recordings from a BAPTA-treated monolayer during application of shocks of variable strength. In all BAPTA-treated cell strands, shocks with strength of ~20 and ~30 V/cm induced arrhythmias that had fewer beats (Figure 5B, $p<0.01$) and lasted shorter time (Figure 5C, $p<0.05$) than in control monolayers. The value of arrhythmia duration caused by 30-V/cm shocks in BAPTA presence is underestimated because these arrhythmias could last longer than the 5-sec recording interval. Average cycle length, measured as arrhythmia duration divided by number of extra beats, was not significantly affected by BAPTA (Figure 5D, NS).

Effects of I_{NCX} and I_{K1} inhibition on arrhythmia duration

To examine the role of I_{NCX} current in shock-induced arrhythmias, the effect of an NCX inhibitor, KB-R7943, on arrhythmia duration was measured using recordings of cell contractions in transmitted light. A series of shocks with strength of approximately 0, 10, 20, 30 and 40 V/cm was applied in control conditions, during KB-R7943 application, and after drug washout. Different cultures exhibited substantial variability in threshold of arrhythmogenic shock strength and arrhythmia duration in control conditions. To limit this variability, analysis of KB-R7943 effects was limited to strands with ~30-V/cm arrhythmia thresholds in control conditions. This group included 12 strands from 6 cell monolayers.

Figure 6A shows optical recordings of cell contractions from a typical cell strand exposed to shocks in control, during KB-R7943 application, and after drug washout. The minor deflections visible after the contractions were caused by vibrations of the solution surface in the perfusion bath. It can be seen that KB-R7943 increased the number of shock-induced arrhythmic beats in comparison to control and that this effect was reversible upon drug washout. Similar results were obtained in other cell strands. For shock strengths of ~30 V/cm and above, KB-R7943 significantly increased the arrhythmia duration and the number of shock-induced arrhythmic beats in comparison to control (Figure 6B). The effect on arrhythmia duration was reversible; after drug washout, it was similar to control for all

shock strengths. Application of KB-R7943 also decreased the mean cycle length, although this effect was not completely reversible after washout.

The KB-R7943 data indicate that Ca_i^{2+}-activated inward NCX current was not the driving force for shock-induced arrhythmias. Moreover, I_{NCX} inhibition unexpectedly prolonged arrhythmias. It can be hypothesized that this effect could be explained by increase of Ca_i^{2+} caused by NCX inhibition and Ca_i^{2+}-dependent reduction of the outward component of the inward rectifier current, I_{K1}, which may destabilize resting membrane potential and promote arrhythmias, as reported previously.[24] The same Ca_i^{2+}-dependent mechanism may also explain arrhythmia duration reduction by BAPTA-AM. To examine the role of I_{K1} in shock-induced arrhythmias, the effect of I_{K1} inhibitor $BaCl_2$ (0.2-mmol/L) on arrhythmia duration was measured in 8 strands from 4 monolayers, which had arrhythmia thresholds ~30 V/cm in control conditions. In each strand, arrhythmia duration was measured using recordings of cell contractions in control, during $BaCl_2$ application, and after drug washout. As shown in Figure 6C, $BaCl_2$ application significantly increased the number of arrhythmic beats compared to control for 30- and 40-V/cm shocks and the arrhythmia duration for 40-V/cm shocks. This effect was reversible; upon $BaCl_2$ washout, both parameters returned to control values. Effect of $BaCl_2$ on average cycle length was less consistent; differences between control and drug-treated measurements were not statistically significant.

DISCUSSION

This study investigated the roles of spontaneous Ca_i^{2+} rises and inward I_{NCX} in shock-induced arrhythmias occurring in neonatal rat myocyte monolayers. The principal findings are: (1) V_m upstrokes preceded Ca_i^{2+} rises at the arrhythmia source, and the V_m-Ca_i^{2+} delay did not differ between arrhythmic and paced beats. Shocks caused gradual Ca_i^{2+} elevation without detectable SCRs preceding arrhythmic action potentials; (2) application of Ca_i^{2+} chelator BAPTA-AM decreased shock-induced arrhythmia duration; (3) NCX inhibition by KB-R7943 increased arrhythmia duration. Effects of both BAPTA-AM and KB-R7943 could be due to Ca_i^{2+}-dependent inhibition of outward I_{K1}. I_{K1} inhibition by $BaCl_2$ increased the arrhythmia duration, providing support for part of this hypothesis.

Mechanism of shock-induced arrhythmias

A common mechanism of focal arrhythmias involves spontaneous Ca^{2+} rise due to ion release from the sarcoplasmic reticulum precipitated by Ca_i^{2+} overload and followed by activation of I_{NCX} and membrane depolarization.[14] Although strong shocks cause diastolic Ca_i^{2+} increase, as reported in previous studies[11,13] and here, two findings of this study indicate that this mechanism was not responsible for shock-induced arrhythmias. First, arrhythmias were not suppressed by NCX inhibition as would be expected if they were caused by activation of inward I_{NCX}. Second, no SCRs were observed. Such SCRs could be detected by measuring negative or very small delays between Ca_i^{2+} transients and APs at the arrhythmia source[17,19] but V_m-Ca_i^{2+} delays were not different between arrhythmic and paced beats in this work. SCRs could also be revealed by slow Ca_i^{2+} rises preceding Ca_i^{2+} transients[18,20,25] but no significant Ca_i^{2+} rises immediately before arrhythmic APs were observed either. Analysis of Ca_i^{2+} signals recorded with and without shocks demonstrated a gradual rise in Ca_i^{2+}. This rise began immediately after shock application indicating that its cause was ion influx via shock-induced membrane pores without additional calcium influxes right before arrhythmic APs.

One can argue that SCRs were not detected because they occurred in individual cells and were averaged out in optical recordings from diodes which imaged an area with dimensions of 110 μm and collected light from several cells. However, Ca_i^{2+} rise in a single cell is unlikely to cause a propagated V_m response in cell monolayers because of the “critical size”

limitation on excitation source.[26] Although critical size of excitation in cell cultures is unknown, the value of electrotonic space constant of ~360 μm[27] suggests that multiple cells must generate SCRs to produce an arrhythmic beat. If present, such SCRs would be detectable here.

Besides spontaneous Ca_i^{2+} rise and I_{NCX} activation, the other probable inward current which could raise V_m and induce arrhythmias is a non-specific leakage current, which flows through membrane pores produced by shocks. Voltage-clamp measurements in isolated cells have shown that large V_m displacements transiently increase membrane conductivity producing non-specific inward leakage current.[9] In non-clamped cells, this current will depolarize the membrane, which may raise V_m to activation threshold causing arrhythmias. Post-shock diastolic depolarization was reported previously in cell cultures,[10,11] tissue preparations,[12,28] and whole hearts.[29] Shock-induced changes in membrane conductivity and diastolic V_m are transient, with both parameters gradually returning to normal values, likely due to gradual pore re-sealing at a rate which is dependent on shock strength. Transient diastolic V_m rise and gradual increase in arrhythmia cycle length observed in the present study are consistent with such membrane changes supporting the role of non-specific leakage current in shock-induced arrhythmias observed in cell cultures.

The role of Ca_i^{2+} in shock-induced arrhythmias

Although the Ca_i^{2+}-dependent mechanism was not the immediate cause of shock-induced arrhythmias, results suggest that Ca_i^{2+} did play a role in arrhythmia maintenance, as indicated by the effect of Ca^{2+} chelator BAPTA, which decreased the arrhythmia duration. This finding suggests that reducing cytoplasmic Ca^{2+} concentration may have an antiarrhythmic effect. The effect of the I_{NCX} inhibitor KB-R7943, which increased the arrhythmia duration, can be explained by the same mechanism, since NCX is responsible for approximately half of Ca^{2+} removal from cytosol in neonatal rat myocytes,[30] and NCX inhibition is likely to increase diastolic Ca_i^{2+} levels.

The mechanism of dependence of shock-induced arrhythmias on Ca_i^{2+} is not clear at this time. A possible explanation is that this mechanism involves the inward rectifier current I_{K1}, which is the primary current responsible for maintaining resting V_m.[31] It is known that I_{K1} loss results in membrane depolarization and may, therefore, facilitate focal arrhythmias. It is also known that Ca_i^{2+} increase reduces outward I_{K1}.[24] Therefore, it can be hypothesized that BAPTA and KB-R7943 affected shock-induced arrhythmias via modulation of Ca_i^{2+} and thus I_{K1}. The possible role of I_{K1} in shock-induced arrhythmias is supported by results of experiments with I_{K1} inhibitor $BaCl_2$, which increased the arrhythmia duration. The link between Ca_i^{2+} changes and I_{K1} under experimental conditions employed in this study remains to be elucidated.

Limitations

Analysis of the V_m-Ca_i^{2+} relationship was limited to first arrhythmic beats with relatively long coupling intervals produced by weak shocks in order to avoid interference from cell contractions. It is possible that this relationship might be different for faster and longer arrhythmias produced by stronger shocks. Channel blockers used here are not entirely specific to their intended targets, which require caution in interpretation of drug experiments. Finally, application of findings obtained in cell cultures to whole adult hearts may be limited by differences in ionic properties, tissue structure, electrophysiological heterogeneities, presence of disease, etc. For example, sarcoplasmic reticulum is less developed,[32,33] NCX expression is larger,[34] and I_{K1} current density is smaller[35] in neonatal myocytes than in adult cells. Therefore, contributions of these channels and SCRs to shock-induced arrhythmias in whole hearts and in neonatal myocyte cultures may differ.

Acknowledgments

The authors thank Shannon Salter for help with growth substrate preparation.

This work was supported by NIH grant HL067748

List of Abbreviations

AP	action potential
APA	AP amplitude
Ca_i^{2+}	intracellular calcium concentration
CaA	amplitude of Ca_i^{2+} transient
E	shock field strength
I_{K1}	inward rectifier current
I_{NCX}	sodium-calcium exchange current
NCX	sodium-calcium exchanger
SCR	spontaneous calcium rise
V_m	membrane potential
ΔV_m	shock-induced V_m change

REFERENCES

1. Dosdall DJ, Fast VG, Ideker RE. Mechanisms of defibrillation. Annu Rev Biomed Eng. 2010; 12:233–258. [PubMed: 20450352]
2. Tung L. Detrimental effects of electrical fields on cardiac muscle. Proceed IEEE. 1996; 84:366–378.
3. Cates AW, Wolf PD, Hillsley RE, Souza JJ, Smith WM, Ideker RE. The probability of defibrillation success and the incidence of postshock arrhythmia as a function of shock strength. PACE. 1994; 17:1208–1217. [PubMed: 7937226]
4. Jones JL, Jones RE. Postshock arrhythmias--a possible cause of unsuccessful defibrillation. Crit Care Med. 1980; 8:167–171. [PubMed: 7363633]
5. Chattipakorn N, Banville I, Gray RA, Ideker RE. Effects of shock strengths on ventricular defibrillation failure. Cardiovasc Res. 2004; 61:39–44. [PubMed: 14732200]
6. Fedorov VV, Kostecki G, Hemphill M, Efimov IR. Atria are more susceptible to electroporation than ventricles: implications for atrial stunning, shock-induced arrhythmia and defibrillation failure. Heart Rhythm. 2008; 5:593–604. [PubMed: 18362029]
7. Cheek ER, Fast VG. Nonlinear changes of transmembrane potential during electrical shocks: role of membrane electroporation. Circ Res. 2004; 94:208–214. [PubMed: 14670844]
8. Fedorov VV, Nikolski VP, Efimov IR. Effect of electroporation on cardiac electrophysiology. Methods Mol Biol. 2008; 423:433–448. [PubMed: 18370220]
9. O'Neill RJ, Tung L. Cell-attached patch clamp study of the electropermeabilization of amphibian cardiac cells. Biophys J. 1991; 59:1028–1039. [PubMed: 1907865]
10. Fast VG, Cheek ER. Optical mapping of arrhythmias induced by strong electrical shocks in myocyte cultures. Circ Res. 2002; 90:664–670. [PubMed: 11934833]
11. Krauthamer V, Jones JL. Calcium dynamics in cultured heart cells exposed to defibrillator-type electric shocks. Life Sciences. 1997; 60:1977–1985. [PubMed: 9180351]
12. Neunlist M, Tung L. Dose-dependent reduction of cardiac transmembrane potential by high-intensity electrical shocks. Am J Physiol. 1997; 273:H2817–H2825. [PubMed: 9435619]
13. Fast VG, Cheek ER, Pollard AE, Ideker RE. Effects of electrical shocks on Ca_i^{2+} and V_m in myocyte cultures. Circ Res. 2004; 94:1589–1597. [PubMed: 15155528]

14. Schlotthauer K, Bers DM. Sarcoplasmic reticulum Ca(2+) release causes myocyte depolarization. Underlying mechanism and threshold for triggered action potentials. Circ Res. 2000; 87:774–780. [PubMed: 11055981]
15. Kass RS, Tsien RW, Weingart R. Ionic basis of transient inward current induced by strophanthidin in cardiac Purkinje fibres. J Physiol. 1978; 281:209–226. [PubMed: 702372]
16. Mechmann S, Pott L. Identification of Na-Ca exchange current in single cardiac myocytes. Nature. 1986; 319:597–599. [PubMed: 2418367]
17. Choi BR, Burton F, Salama G. Cytosolic Ca2+ triggers early afterdepolarizations and Torsade de Pointes in rabbit hearts with type 2 long QT syndrome. J Physiol. 2002; 543:615–631. [PubMed: 12205194]
18. Hoeker GS, Katra RP, Wilson LD, Plummer BN, Laurita KR. Spontaneous calcium release in tissue from the failing canine heart. Am J Physiol. 2009; 297:H1235–H1242.
19. Nemec J, Kim JJ, Gabris B, Salama G. Calcium oscillations and T-wave lability precede ventricular arrhythmias in acquired long QT type 2. Heart Rhythm. 2010; 7:1686–1694. [PubMed: 20599524]
20. Maruyama M, Joung B, Tang L, et al. Diastolic intracellular calcium-membrane voltage coupling gain and postshock arrhythmias: role of purkinje fibers and triggered activity. Circ Res. 2010; 106:399–408. [PubMed: 19926871]
21. Rohr S, Fluckiger-Labrada R, Kucera JP. Photolithographically defined deposition of attachment factors as a versatile method for patterning the growth of different cell types in culture. Pflugers Arch. 2003; 446:125–132. [PubMed: 12690471]
22. Fast VG, Rohr S, Ideker RE. Non-linear changes of transmembrane potential caused by defibrillation shocks in strands of cultured myocytes. Am J Physiol. 2000; 278:H688–H697.
23. Fast VG, Ideker RE. Simultaneous optical mapping of transmembrane potential and intracellular calcium in myocyte cultures. J Cardiovasc Electrophysiol. 2000; 11:547–556. [PubMed: 10826934]
24. Delmar M, Ibarra J, Davidenko J, Lorente P, Jalife J. Dynamics of the background outward current of single guinea pig ventricular myocytes. Ionic mechanisms of hysteresis in cardiac cells. Circ Res. 1991; 69:1316–1326. [PubMed: 1934360]
25. Katra RP, Laurita KR. Cellular mechanism of calcium-mediated triggered activity in the heart. Circ Res. 2005; 96:535–542. [PubMed: 15718502]
26. Fast VG, Kleber AG. Role of wavefront curvature in propagation of cardiac impulse. Cardiovasc Res. 1997; 33:258–271. [PubMed: 9074688]
27. Jongsma HJ, van Rijn HE. Electrotonic spread of current in monolayer cultures of neonatal rat heart cells. J Membrane Biol. 1972; 9:341–360. [PubMed: 4640972]
28. Kodama I, Shibata N, Sakuma I, et al. Aftereffects of high-intensity DC stimulation on the electromechanical performance of ventricular muscle. Am J Physiol. 1994; 267:H248–H258. [PubMed: 7519406]
29. Nikolski VP, Sambelashvili AT, Krinsky VI, Efimov IR. Effects of electroporation on optically recorded transmembrane potential responses to high-intensity electrical shocks. Am J Physiol. 2004; 286:H412–H418.
30. Bers, DM. Excitation-Contruction Coupling and Cardiac Contractile Force. 2nd ed.. Norwell, MA: Kluwer Academic Publishers; 2001.
31. Lopatin AN, Nichols CG. Inward rectifiers in the heart: an update on I(K1). J Mol Cell Cardiol. 2001; 33:625–638. [PubMed: 11273717]
32. Cohen NM, Lederer WJ. Changes in the calcium current of rat heart ventricular myocytes during development. J Physiol. 1988; 406:115–146. [PubMed: 2855434]
33. Wibo M, Bravo G, Godfraind T. Postnatal maturation of excitation-contraction coupling in rat ventricle in relation to the subcellular localization and surface density of 1,4-dihydropyridine and ryanodine receptors. Circ Res. 1991; 68:662–673. [PubMed: 1660357]
34. Boerth SR, Zimmer DB, Artman M. Steady-state mRNA levels of the sarcolemmal Na(+)-Ca2+ exchanger peak near birth in developing rabbit and rat hearts. Circ Res. 1994; 74:354–359. [PubMed: 8293573]

35. Wahler GM. Developmental increases in the inwardly rectifying potassium current of rat ventricular myocytes. Am J Physiol. 1992; 262:C1266–C1272. [PubMed: 1590363]

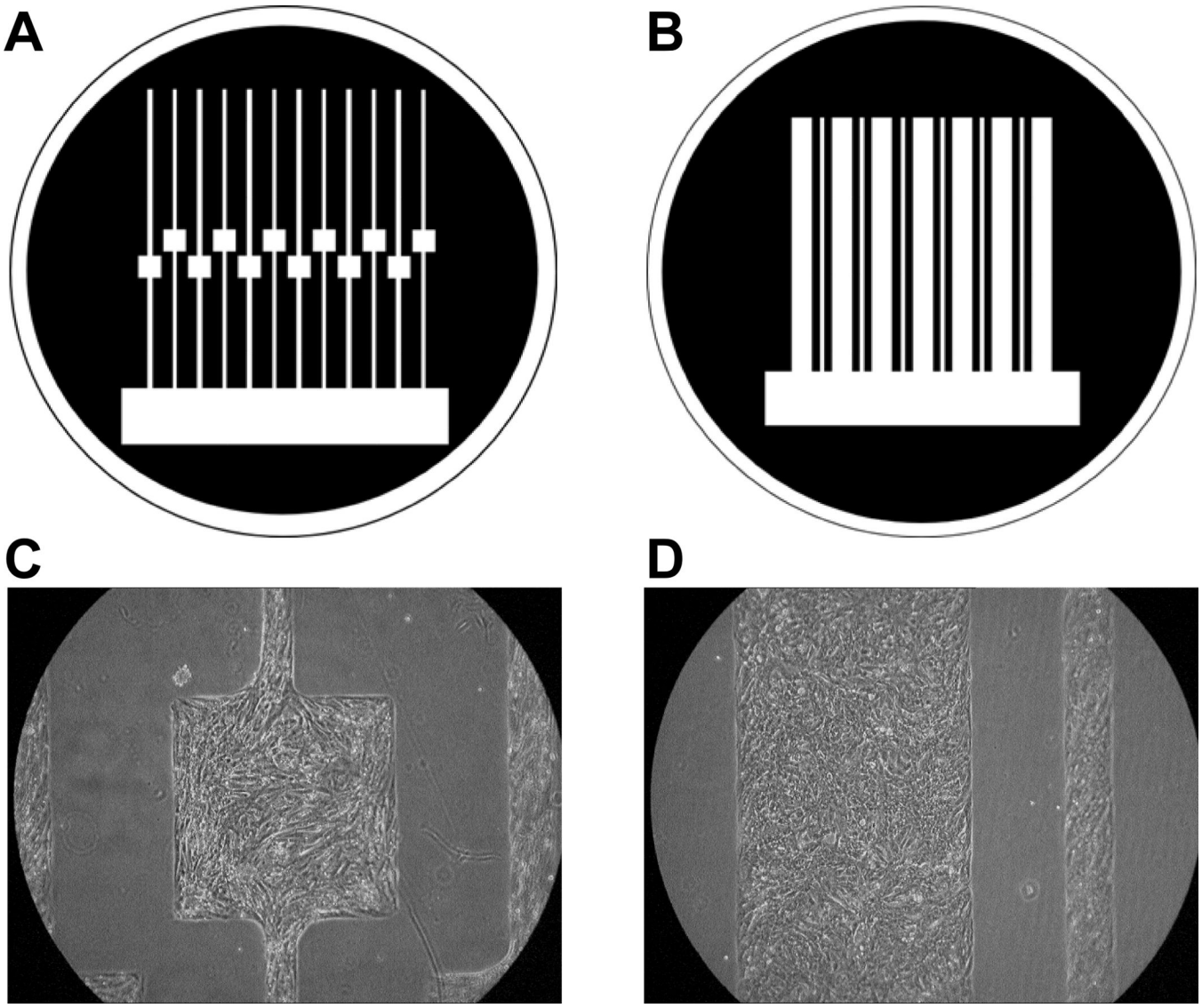

Figure 1.

Preparation of patterned growth cell cultures. **A–B**, Photolithographic masks used for patterned growth. The first (A), consisted of narrow strands (width=0.15 mm) containing an area of local expansion (width=0.8 mm); the second (B), consisted of linear cell strands with widths of 0.2 and 0.8 mm. Areas of cell growth are shown in white. **C–D**, Examples of patterned cultures of neonatal rat ventricular myocytes.

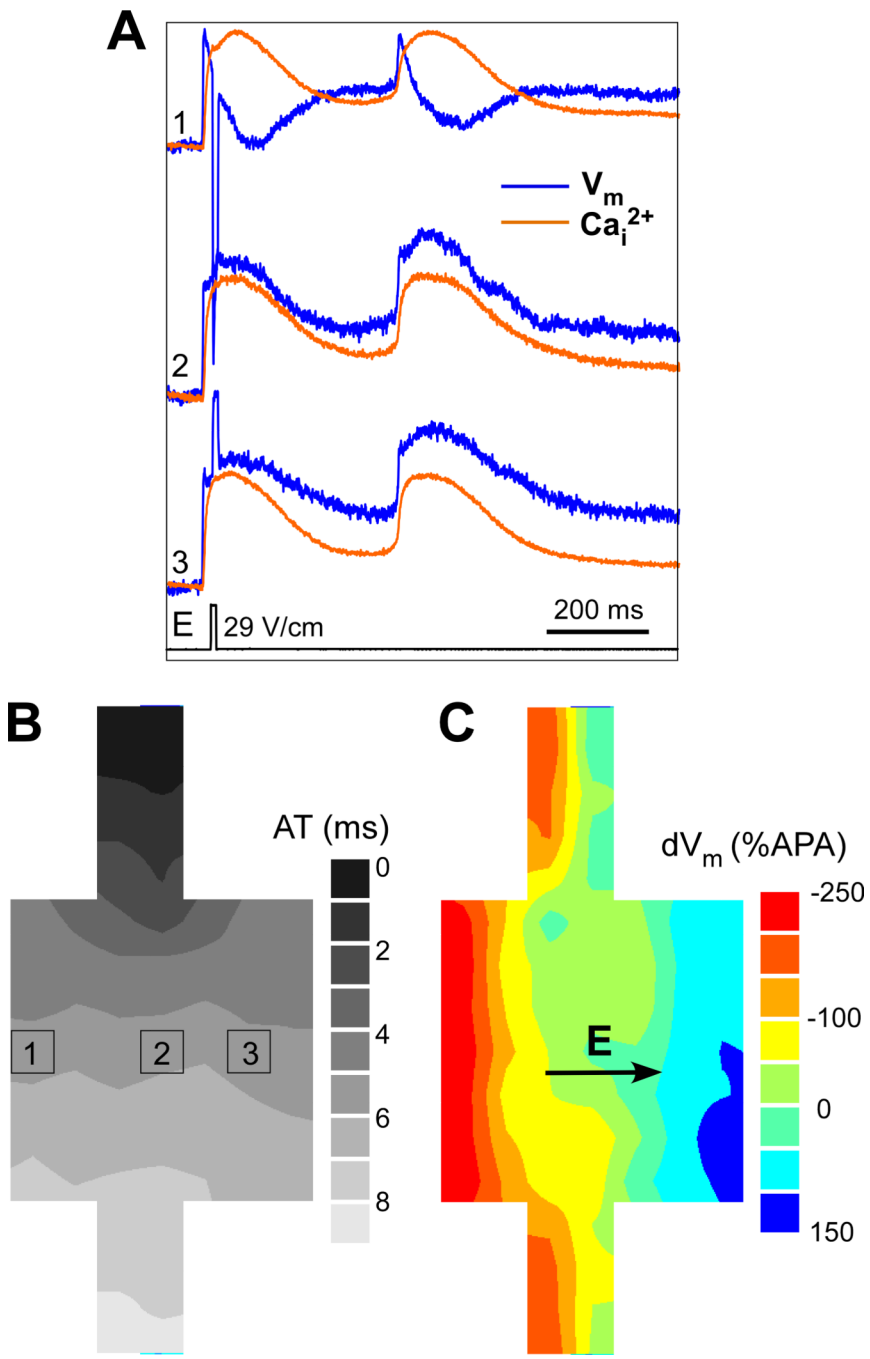

Figure 2.

Effects of shock application on V_m and Ca_i^{2+}. **A**, Simultaneous recordings of V_m and Ca_i^{2+} during application of 29-V/cm shock, which induced one arrhythmic beat. **B**, Isochronal map of activation spread during the paced beat. **C**, Isopotential map of maximal shock-induced ΔV_m distribution.

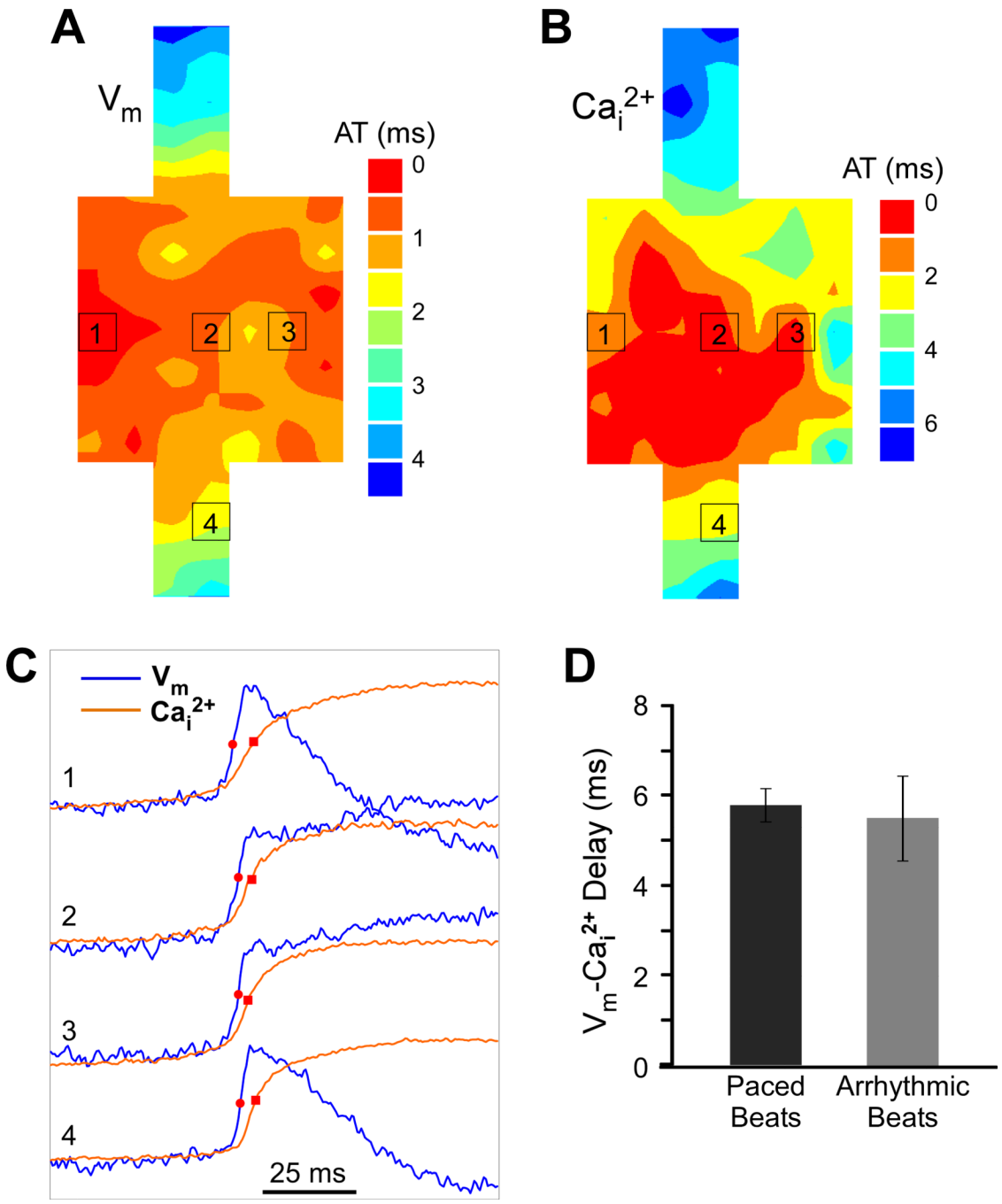

Figure 3.

Relationship between V_m and Ca_i^{2+} rises during an arrhythmic beat. **A**, Isochronal map of activation spread during the arrhythmic beat. AT, activation time. **B**, Isochronal map of Ca_i^{2+} spread during the arrhythmic beat. **C**, V_m and Ca_i^{2+} recordings from selected sites within the expansion region (sites 1–3) and the narrow strand (site 4). **D**, Comparison of average V_m-Ca_i^{2+} delay between arrhythmic and paced beats.

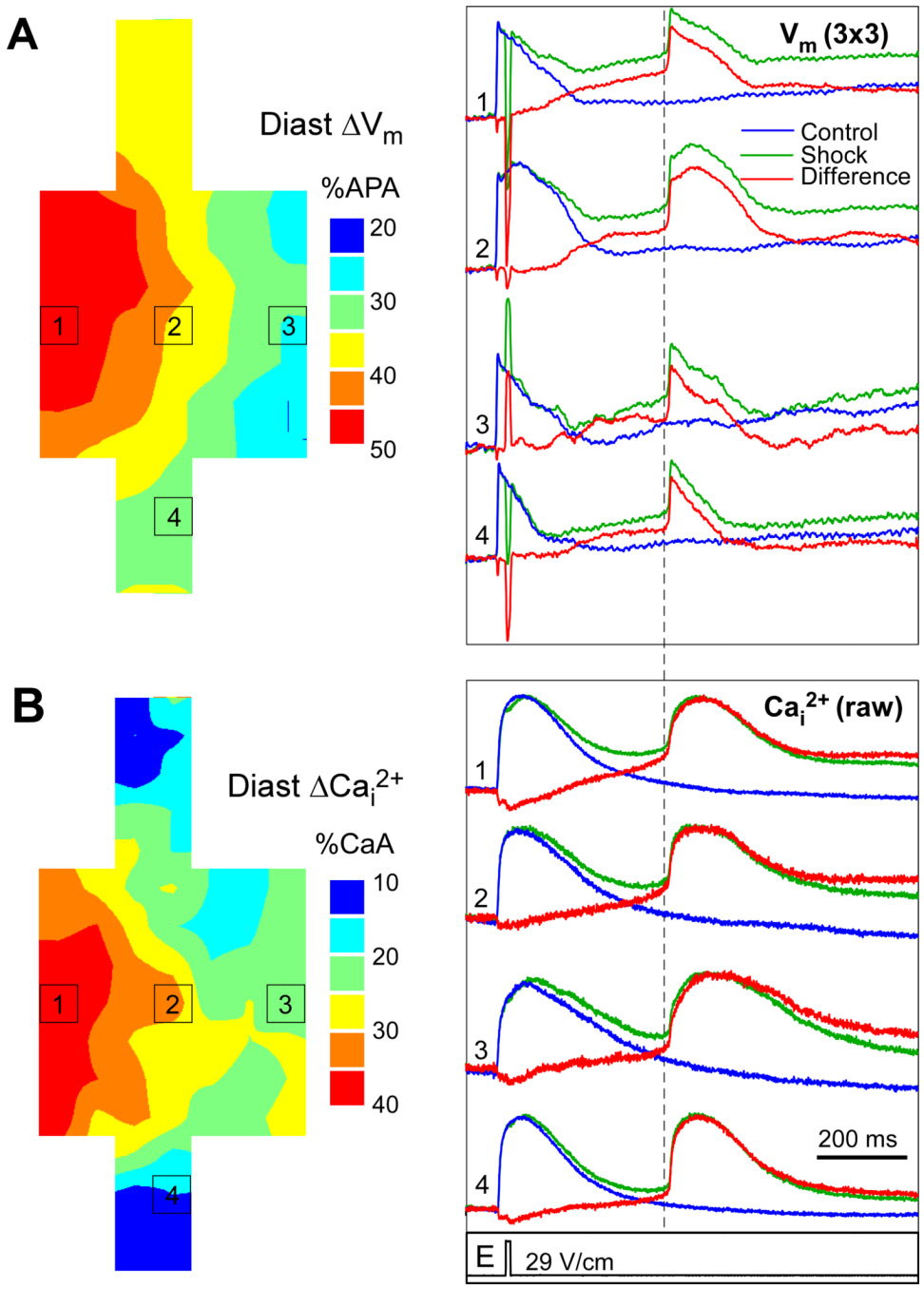

Figure 4.

Post-shock elevation of V_m and Ca_i^{2+}. **A**, Isochronal map of diastolic ΔV_m and spatially averaged V_m traces from control (blue) and shock (green) recordings, as well as the difference between shock and control (red). **B**, Isochronal map of diastolic Ca_i^{2+} rises and selected raw signals showing control, shock, and difference recordings. The dashed line indicates the measurement point of diastolic levels.

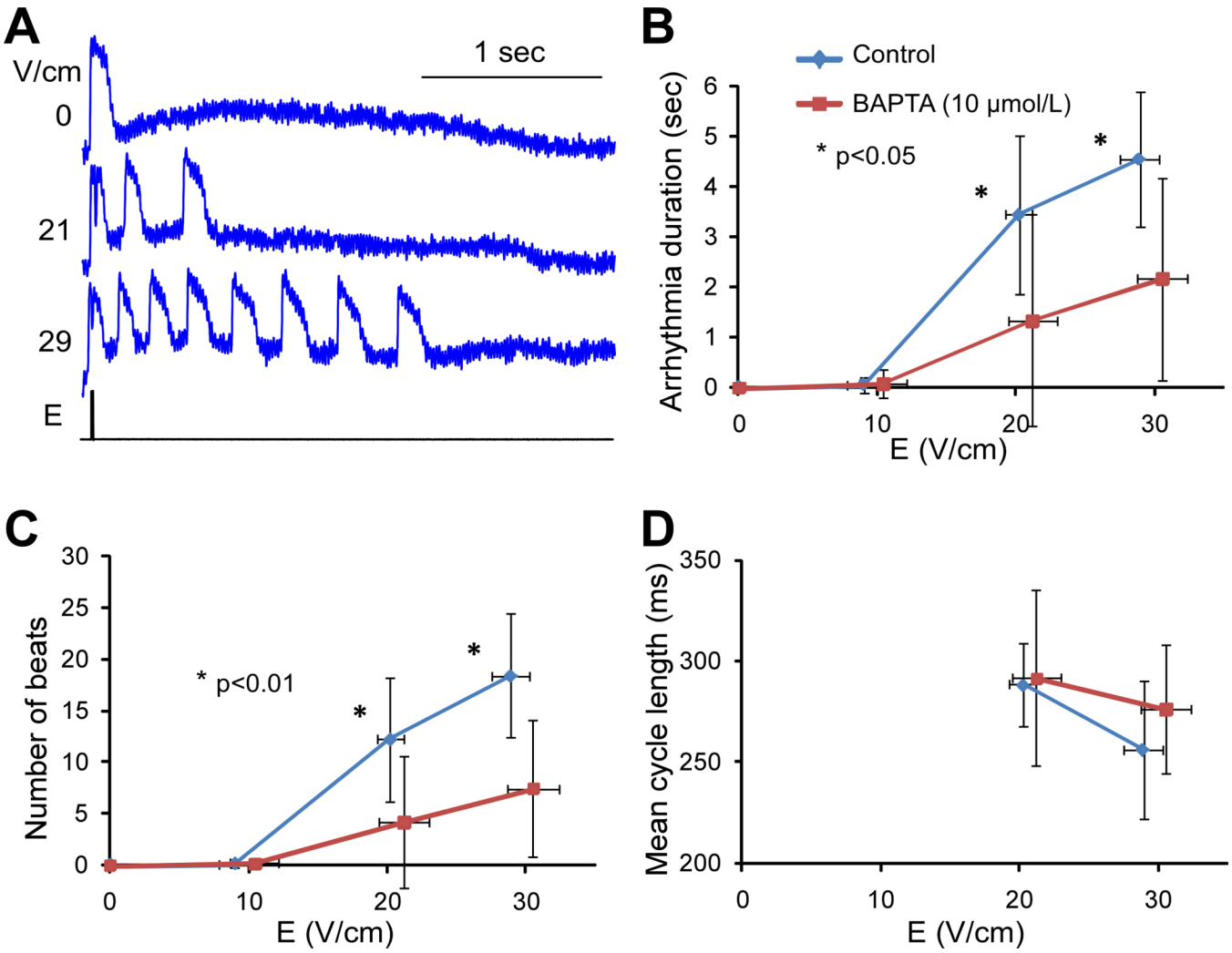

Figure 5.

Effect of BAPTA on arrhythmias. **A**, V_m traces recorded during shock application of different strengths in a BAPTA-treated monolayer. **B**, Arrhythmia duration measured during 5-sec interval in control strands (n=9) and BAPTA-treated strands (n=17). **C**, Number of arrhythmic beats. **D**, Average cycle length of arrhythmic beats measured as the ratio between arrhythmia duration and number of beats.

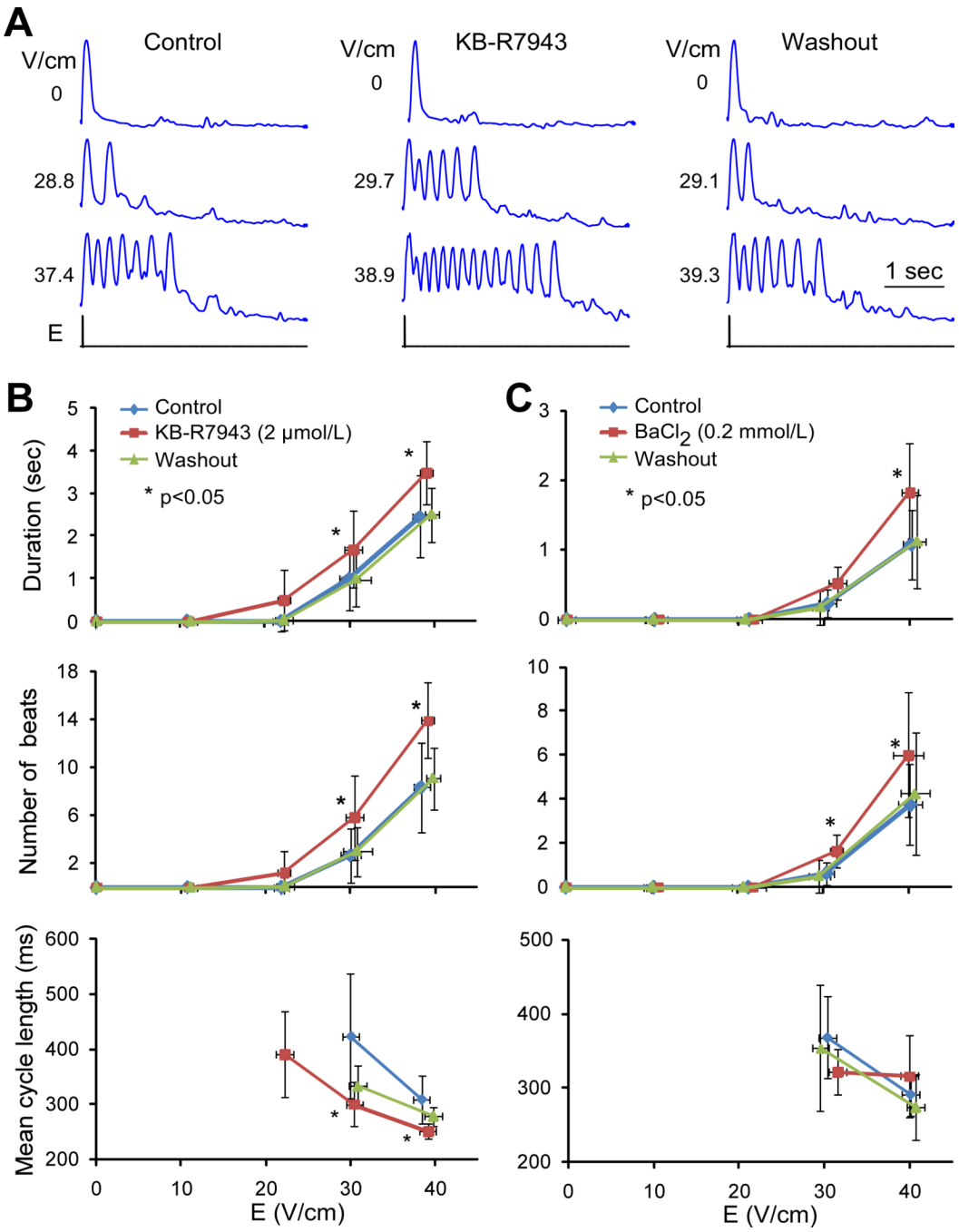

Figure 6.

Effect of KB-R7943 and $BaCl_2$ on arrhythmias. **A**, Recordings of cell contractions in response to different shock strengths and experimental treatment. **B** and **C**, Arrhythmia duration, number of beats, and their average cycle length measured during 5-sec interval in 12 cell strands in control, during KB-R7943 application, and after drug washout. **C**, Respective parameters measured in 8 cell strands in control, during BaCl2 application, and after drug washout.